Earth's Future

RESEARCH ARTICLE
10.1029/2024EF004489

Increasing Optimum Temperature of Vegetation Activity Over the Past Four Decades

Yiheng Wang[1,2], Sangeeta Sarmah[1], Mrinal Singha[3], Weinan Chen[1,2], Yong Ge[4], Liyin L. Liang[5], Santonu Goswami[6], and Shuli Niu[1,2]

[1]Key Laboratory of Ecosystem Network Observation and Simulation, Institute of Geographical Sciences and Natural Resources Research, Chinese Academy of Sciences, Beijing, China, [2]School of Resources and Environment, University of Chinese Academy of Sciences, Beijing, China, [3]Indian Institute of Human Settlements (IIHS), Bangalore, Karnataka, India, [4]State Key Laboratory of Resources and Environmental Information Systems, Institute of Geographic Sciences & Natural Resources Research, Chinese Academy of Sciences, Beijing, China, [5]Manaaki Whenua - Landcare Research, Palmerston North, New Zealand, [6]Center for Climate Change and Sustainability, Azim Premji University Bangalore, Bangalore, Karnataka, India

Key Points:

- The optimum temperature (T_{opt}) of global vegetation activity has increased rapidly, by 0.63 per decade over 1982–2020
- The increase in T_{opt} closely tracked the increase in air temperature, revealing widespread thermal acclimation across global vegetation
- Continental and polar ecosystems showed the greatest capacity for acclimation

Supporting Information:

Supporting Information may be found in the online version of this article.

Correspondence to:

S. Niu,
sniu@igsnrr.ac.cn

Citation:

Wang, Y., Sarmah, S., Singha, M., Chen, W., Ge, Y., Liang, L. L., et al. (2024). Increasing optimum temperature of vegetation activity over the past four decades. *Earth's Future*, *12*, e2024EF004489. https://doi.org/10.1029/2024EF004489

Received 22 FEB 2024
Accepted 29 AUG 2024

Author Contributions:

Conceptualization: Yiheng Wang, Sangeeta Sarmah, Shuli Niu
Formal analysis: Yiheng Wang, Sangeeta Sarmah, Mrinal Singha
Investigation: Yiheng Wang, Shuli Niu
Methodology: Yiheng Wang, Sangeeta Sarmah, Shuli Niu
Project administration: Shuli Niu
Software: Yiheng Wang, Mrinal Singha
Supervision: Shuli Niu
Visualization: Yiheng Wang
Writing – original draft: Yiheng Wang, Sangeeta Sarmah
Writing – review & editing: Yiheng Wang, Weinan Chen, Yong Ge, Liyin L. Liang, Santonu Goswami, Shuli Niu

Abstract Over the past four decades, global temperatures have increased more rapidly than before, potentially reducing vegetation activity if temperatures exceed the optimum temperature (T_{opt}). However, plants have the capacity to acclimate to rising temperatures by adjusting T_{opt}, thereby maintaining or even enhancing photosynthesis and carbon uptake. Despite this, it remains unclear how T_{opt} of vegetation activity changes over time and to what extent global vegetation can acclimate to current temperature changes. In this study, we evaluated the temporal trends of T_{opt} of vegetation activity and the thermal acclimation magnitudes globally using three remote-sensed vegetation indices and eddy-covariance observations of gross primary productivity from 1982 to 2020. We found that the global T_{opt} of vegetation activity has increased at an average rate of 0.63°C per decade over the past four decades. The increase in T_{opt} closely tracked the rise in annual maximum daily mean temperature (T_{max}), indicating that thermal acclimation has occurred widely across the globe. Globally, we found an average thermal acclimation magnitude of 0.38°C per 1°C increase in T_{max}. Notably, polar and continental regions exhibited the highest thermal acclimation magnitudes, while arid areas showed the lowest. Additionally, the thermal acclimation magnitude was positively affected by interannual temperature variability and negatively affected by soil moisture and vapor pressure deficits. Our findings indicate that terrestrial ecosystems have acclimated to current climate warming trends with varying degrees, suggesting a greater potential for land carbon uptake. Moreover, these results highlight the necessity for earth system models to integrate the thermal acclimation of T_{opt} to better forecast the global carbon cycle.

Plain Language Summary Global warming affects vegetation growth, and plants may acclimate to temperature changes to enhance their growth and activity. However, how effectively global vegetation can adjust to temperature changes is unclear. To examine this, we analyzed satellite and ground data from 1982 to 2020 to determine changes in the optimum temperature of vegetation activity. We found that global vegetation has acclimated to rising temperatures by increasing the optimum temperatures. Polar and continental vegetation have undergone the greatest acclimation. In addition, ecosystems with humid climates and higher temperature variability have a greater capacity to acclimate to rising temperatures. These findings have important implications for better predicting how warming will affect the global carbon cycle.

1. Introduction

Understanding the temperature response of vegetation activity is critical for anticipating the response of global ecosystems to warming and their feedback to climate change (Hughes, 2000; Niu et al., 2008; Smith & Dukes, 2013). The temperature response curves at both the leaf and ecosystem levels have shown that plant photosynthesis and ecosystem productivity typically increase with temperature up to an optimum temperature (T_{opt}) (Huang et al., 2019; Lloyd & Farquhar, 2008) before they rapidly decline due to impairments in electron-transport and Rubisco enzymatic capacity, stomatal regulation, and accelerated leaf senescence (Grossiord et al., 2020; Niinemets, 2001; Scafaro et al., 2017). In recent decades, land temperatures have risen at a faster rate than in the preceding century (Masson-Delmotte et al., 2021). This accelerated warming rate is expected to

influence plant activity and temperature responses (Saxe et al., 2001; Smith et al., 2017). However, the corresponding changes in T_{opt} of vegetation activity have not been comprehensively investigated.

Plants can adjust their temperature response and increase their T_{opt} in response to rising temperatures, a phenomenon known as thermal acclimation (Smith et al., 2016; Yamori et al., 2014). Thermal acclimation of photosynthesis has been widely observed at the leaf level (Smith & Dukes, 2013; Yamori et al., 2014), and warming experiments show that plants can increase their T_{opt} for leaf photosynthesis with growth temperatures by up to 10°C (Battaglia et al., 1996). However, recent studies indicate that the T_{opt} for vegetation activity at the ecosystem scale differed significantly from leaf-level observations (Huang et al., 2019). Nevertheless, it remains unclear whether thermal acclimations occur at the ecosystem level. Previous studies reported that ecosystem T_{opt} increased with annual maximum daily temperature (T_{max}) at a spatial scale and hypothesized that the temporal acclimation in T_{opt} to increasing temperatures would mirror this spatial sensitivity (Huang et al., 2018; Wang et al., 2023). However, it is unclear whether the spatial sensitivity accurately reflects the temporal responses of T_{opt} to T_{max} and whether thermal acclimations have already occurred under the current warming levels. Moreover, the capacity for thermal acclimation differs considerably among plant species. For instance, previous studies showed that tropical and subtropical forest species had a greater acclimation capacity than temperate species (Choury et al., 2022). Similarly, the thermal acclimation capacity also varied greatly among photosynthetic pathways (C_3, C_4, and CAM) and functional types that differ in their distributions (Tjoelker et al., 1998; Yamori et al., 2014). Despite this, how thermal acclimation capacity differs among various biomes and climatic regions remains unknown. Accessing the thermal acclimation capacity of global ecosystems is crucial for predicting future changes in T_{opt} and terrestrial carbon uptake.

The ability of plants to acclimate to elevated temperatures appears to be intricately linked to their background climate (Crous et al., 2022; Kumarathunge et al., 2019). For example, species that experience a more variable environment have been found to acclimate better to increased growth temperature than those living in a stable environment (Björkman et al., 1978; Cunningham & Read, 2002). In addition, a recent study showed that ecosystems in humid and cold regions acclimated more rapidly to temperature changes than those in dry and warm areas (Wang et al., 2023). However, it is challenging to synthesize and compare the drivers of acclimation capacity and how they regulate the temperature response of plants (Lin et al., 2012). To address these knowledge gaps, we investigated the temporal trends of T_{opt} of vegetation activity and determined the thermal acclimation magnitudes of global vegetation using long-term remote sensing data sets of three vegetation indices during 1982–2020 and ground observations from 132 eddy-covariance sites. Specifically, we aimed to address the following questions: (a) Does the global T_{opt} demonstrate an increasing trend over the past four decades? (b) To what extent has global vegetation acclimated to current temperature changes, and how do the thermal acclimation magnitudes differ among biomes and climate zones, and (c) Which environmental or biotic factors primarily influence the thermal acclimation magnitude?

2. Materials and Methods

2.1. Data

Our study aimed to evaluate the changes in T_{opt} of vegetation activity during 1982–2020 across global vegetated areas. Vegetated areas were defined as regions where the annual mean Normalized Difference Vegetation Index (NDVI) > 0.1 (Figure S1 in Supporting Information S1, Fang et al., 2004). We used three types of vegetation indices derived from satellite observations to investigate the temporal variations of T_{opt}, including daily NDVI, near-infrared reflectance of vegetation (NIRv), and gross primary productivity (GPP). The NDVI employs the contrast in reflectance between the infrared and red portions of the electromagnetic spectrum, demonstrating a strong correlation with vegetation growth and photosynthesis (Beck et al., 2011). The NDVI demonstrated greater simplicity, accessibility, and historical availability than most other indices, and has been widely used in studies of vegetation dynamics and warming responses (Huang et al., 2018; Lian et al., 2021; Piao et al., 2020). We derived the daily NDVI data set from the Advanced Very High-Resolution Radiometer (AVHRR) sensor by the National Oceanic and Atmospheric Administration (NOAA). The AVHRR NDVI covers 1981 to the present day, with a spatial resolution of 8 km and a temporal resolution of one day (Vermote et al., 2014). The NIRv is a recently developed index for vegetation photosynthesis that is highly sensitive to canopy development, plant phenology, and productivity (Badgley et al., 2017; Wang et al., 2020; Zhang et al., 2022). Daily NIRv was calculated as the product of AVHRR daily NDVI and near-infrared (NIR) reflectance (Pedelty et al., 2007), following Badgley

et al. (2017). A value of 0.08 was subtracted from the NDVI to minimize the influence of soil conditions. Moreover, spatial gaps in AVHRR NDVI and NIRv (e.g., caused by dense cloud cover) were gap-filled using linear interpolation methods (Chen et al., 2004). In addition, daily AVHRR NDVI and NIRv exhibited a few significant errors during the non-growing seasons, showing unusually high values (e.g., Figure S2 in Supporting Information S1). Consequently, all the outliers (i.e., values outside of the median of NDVI/NIRv ±3 times the median absolute deviation) during the non-growing seasons were removed. Finally, we also incorporated FLUXCOM GPP, which was upscaled from local GPP observations of FLUXNET sites through machine learning methods with remote-sensing data and forced by CRUNCEPv6 climate setups (Jung et al., 2017, 2020; Tramontana et al., 2016). The FLUXCOM GPP data sets have a temporal resolution of one day and a spatial resolution of 0.5°, covering 1980–2013. The three products span over 30 years and provided daily observations, allowing the construction of temperature response curves and the extractions of annual T_{opt} for each grid.

We used NASA's MERRA2 reanalyzed daily air temperature data set to extract T_{opt} for vegetation activities at the global scale (Global Modeling and Assimilation Office, 2015). The daily mean temperature from the MERRA2 data set was obtained from Earth DATA. Moreover, to evaluate the T_{opt} trends across different biomes and climatic zones, we used the KÖPPEN-GEIGER climate classification map (Kottek et al., 2006) and MODIS land use/cover (MCD12Q1 V061) product (Sulla-Menashe & Friedl, 2018). The KÖPPEN-GEIGER climate map classifies the globe into five main climatic zones: Arid, Tropical, Humid Temperate, Dry Temperate, Continental, and Polar. Meanwhile, we classified global biomes into nine International Geosphere-Biosphere Programme (IGBP) classes using MODIS land cover data set, including evergreen needleleaf forests (ENF), evergreen broadleaf forests (EBF), deciduous needleleaf forests (DNF), deciduous broadleaf forests (DBF), savannas (SAV), shrublands (SHR), croplands (CRO), grasslands (GRA), and mixed forests (MF). Detailed classification methods, distributions, and zonal climates for different climate zones and biomes are provided Tables S1 and S2, Figures S3, and S4 in Supporting Information S1. Furthermore, we also combined the IGBP and KÖPPEN-GEIGER climate classification to investigate the differences in the T_{opt} trends between different climate backgrounds within a biome (Table S3 in Supporting Information S1).

In addition to satellite observations, we also examined T_{opt} trends across 132 eddy covariance sites (Table S1 in Supporting Information S1) over 1990–2014 using daily GPP (GPP_DT_VUT_REF) and temperature (TA_F) data derived from the FLUXNET 2015 data set (Pastorello et al., 2020). The GPP was estimated from the net ecosystem exchange (NEE) using a daytime partition method. To ensure the high quality of flux site observations, we used daily temperature and GPP data, with at least 50% of the values directly measured or well gap-filled (TA_F_QC and NEE_VUT_REF_QC > 0.5).

To identify the factors influencing the spatial variations of T_{opt} acclimation magnitudes (Muñoz-Sabater et al., 2021) while ensuring data dependency, we used the ERA-5 land product. A total of six climatic variables were derived from the ERA-5 land product, including mean annual temperature (MAT), precipitation (MAP), solar radiation (NSR), vapor pressure deficit (VPD), soil water content (SWC), and interannual variability of temperature (coefficient of variations, CV). Here, CV represents the degree of variation of MAT for each grid over the study period. In addition, we incorporated a potential biotic driver, the leaf area index (LAI), and two soil-related factors, including total soil nitrogen (SOILN) and carbon (SOILC), to evaluate whether these biotic and soil characteristics influence the acclimation capacity of vegetation. Long-term mean LAI was derived from the MODIS LAI product, while the SOILN and SOILC data were derived from the global soil grid data set. All the data sets we used were listed in Table 1 and resampled to the same spatial resolution of 0.5°.

2.2. Estimation of Optimum Temperature (T_{opt}) of Vegetation Activity

We employed two methods to extract the T_{opt} of vegetation activity: the nonlinear regression method and the binned method (Huang et al., 2019). The nonlinear regression method estimates T_{opt} based on the nonlinear relationship between vegetation activity and temperature. For instance, the T_{opt} for NDVI in each grid year was determined by fitting the NDVI-temperature curve using a nonlinear formula derived from the photosynthesis-temperature relationship (Battaglia et al., 1996; Sendall et al., 2015),

$$NDVI(T) = NDVI_{opt} - b(T - T_{opt})^2 + \varepsilon$$

Table 1
Data Sets Used in the Study

Data set	Period	Spatial resolution	Temporal resolution	Accessed
AVHRR NDVI, version 5	1982–2020	0.05°	Daily	NOAA
AVHRR NIR	1982–2020	0.05°	Daily	NOAA
FLUXCOM GPP	2001–2021	0.5°	Daily	FLUXCOM
Temperature	1982–2020	0.25°	Daily	NASA
ERA-5 land product	1982–2020	2.5 arc min	Monthly	ERA-5
MODIS LAI	2001–2020	0.05°	Monthly	NASA LPDAAC
Soilgrid 2.0	–	250 m	–	Poggio et al. (2021)
KÖPPEN-GEIGER climate classification map	2020	0.5°	–	FAO
MODIS Landcover type (MCD12Q1 V6)	2020	1000 m	Yearly	NASA LPDAAC

where NDVI(T) is the NDVI value at a daily mean temperature T, T is the daily mean temperature, ε is the random error, and $NDVI_{opt}$, b, and T_{opt} are parameters to be estimated. Nonlinear regression uses an iterative algorithm to identify the best-fitting model by minimizing the sum of squared errors between the observed data and the model predictions. This process requires an initial starting value for each parameter in the model to initiate the iterations. For each site year, we used the peak NDVI as the initial starting value for $NDVI_{opt}$, the corresponding daily temperature for $T_{opt,}$ and 0 for parameter b. We applied the same method to obtain the T_{opt} for GPP and NIRv globally using FLUXCOM GPP and AVHRR NIRv, respectively.

The binned method determined T_{opt} using four steps: (a) The daily mean temperature data were binned in 1°C increments for each grid year. (b) The daily mean temperature and corresponding NDVI were averaged in each temperature bin. In order to minimize the impact of biotic and human disturbance, we used 95% of the NDVI values in each bin. (c) We calculated the running means of every three temperature bins to construct the temperature response curves of NDVI. (d) T_{opt} was determined from the response curve at which the NDVI reached its maximum value. It is worth noting that T_{opt} may not be captured if the maximum NDVI occurs at the end of the response curves, accounting for 7% of all vegetated areas. In addition, the binned method was applied to derive T_{opt} for GPP at the site level for 132 FLUXNET sites.

To test the robustness of the nonlinear method, we compared the T_{opt} values derived using the nonlinear method with the observed site-level T_{opt} values for GPP. The results showed that NDVI, NIRv, and FLUCOM GPP-derived T_{opt} using nonlinear methods was highly comparable with site observations, with R^2 values of 0.53, 0.28, and 0.88, respectively, and $p < 0.001$ (Figure S5 in Supporting Information S1). In addition, the T_{opt} derived using NDVI and nonlinear method exhibited a similar global pattern to that observed in the previous study (Figure S6 in Supporting Information S1) (Huang et al., 2019). Moreover, we tested whether other climatic factors would affect the accuracy of T_{opt} estimations by constructing a partial model between NDVI and temperature with radiation and precipitation effects excluded. The T_{opt} derived from the partial model aligns with those derived from the nonlinear model ($R^2 = 0.93$, $p < 0.001$) at the 132 FLUXNET sites (Figure S7 in Supporting Information S1), indicating that precipitation and radiation do not affect the T_{opt} for NDVI. Overall, these analyses indicate that the T_{opt} derived by the nonlinear method accurately captures the temperature optimal for plant activity and thus could be used in detecting the changes in T_{opt} over time. The nonlinear model successfully estimated T_{opt} in 93.2% of vegetated areas, while other pixels did not exhibit a parabolic NDVI-temperature curve.

2.3. Statistical Analysis

To evaluate the temporal changes in T_{opt} for vegetation activity from 1982 to 2020, we conducted ordinary least squares regression of T_{opt} for NDVI, NIRv, and GPP against year for each grid, respectively. Additionally, T_{opt}

trends were evaluated on a global scale and within various biomes and climate zones. Moreover, at the site level, we assessed the T_{opt} trends across FLUXNET sites using linear mixed models, with sites serving as random variables. In addition, we also examined the T_{opt} trends at each flux site using median-based linear models, which minimized the impact of extreme values (Rousseeuw, 1984).

To investigate how T_{opt} changes in response to rising temperatures, we calculated partial Pearson correlations between T_{opt} and maximum daily mean temperature (T_{max}) for each grid across the year, by removing the effects of mean annual precipitation and solar radiation changes on T_{opt} using the *R* package *psych* (Revelle & Revelle, 2015). Moreover, we further determined the magnitudes of T_{opt} acclimation to T_{max} changes (thermal acclimation magnitudes) of each grid as the partial regression slope between T_{opt} and T_{max} ($\delta T_{opt}/\delta T_{max}$) across years. We used a linear model ($T_{opt} = T_{max}$ + precipitation + solar radiation) to calculate the partial regression slopes to remove the potential impacts of other climatic factors. Additionally, we also calculated the acclimation magnitudes using T_{opt} and the mean daily maximum temperature in each grid to test the robustness of our results.

To determine the factors that contribute to the spatial variation in thermal acclimation magnitude, we employed a random forest approach. Specifically, we constructed a random forest model to regress thermal acclimation magnitude against a number of climatic and biotic factors. The relative importance of each factor in determining acclimation magnitudes was calculated by dividing its importance in the random forest model by the largest importance value. Additionally, the relationships between the key factors and the acclimation magnitudes were investigated using partial regression methods. All analyses were conducted in *R* using the *mblm*, *nlme*, and *randomForest* packages (Komsta, 2013; Pinheiro et al., 2017; RColorBrewer & Liaw, 2018).

3. Results

3.1. Increasing T_{opt} Over the Last Four Decades

We observed significant increases in the T_{opt} for vegetation activity at regional, biome, and global scales from 1982 to 2020 (Figures 1a and 1b). On a global scale, the mean T_{opt} for AVHRR NDVI has increased by 0.63°C per decade over the past four decades ($R^2 = 0.76$, $p < 0.001$). 20.2% of global vegetated areas showed significant rises in T_{opt} ($p < 0.05$), while 3.3% exhibited significant decreases. The most pronounced increases were observed in Northern Asia, South America, and Central Africa. Similarly, a large proportion of Europe, Asia, and North America also experienced rapid increases in T_{opt}. The T_{opt} derived by the binned method showed consistent increasing trends of T_{opt} (Figure S8 in Supporting Information S1), with a slope of 0.03°C yr^{-1} ($R^2 = 0.47$, $p < 0.001$).

To test the robustness of T_{opt} trends, we conducted additional analyses using AVHRR NIRv, FLUXCOM GPP, and ground-based GPP observations, respectively. The T_{opt} of NIRv and GPP showed consistent increases with that of NDVI (Figures S9 and S10 in Supporting Information S1). Specifically, T_{opt} for AVHRR NIRv exhibited an increase of 0.03°C ($R^2 = 0.46$, $p < 0.001$) per year, while T_{opt} for FLUXCOM GPP showed an increase of 0.02°C per year. In addition, the global patterns of T_{opt} changes for the two indices were similar to that of NDVI. Moreover, ground-based T_{opt} for GPP also yielded comparable results, showing an overall increase in T_{opt} of 0.10°C per year ($p = 0.003$) (Figure S11 in Supporting Information S1). However, due to the limited time coverage of each site (ranging from 3 to 15 years), the T_{opt} trends were less significant for individual sites. Furthermore, we compared the NDVI-derived slopes of T_{opt} with those derived from ground-based GPP for 66 long-term sites (time coverage >5 years), and found highly consistent results ($R^2 = 0.56$, $p < 0.001$), indicating that the increasing rate of T_{opt} for vegetation activity was comparable between site- and satellite-observations (Figure S12 in Supporting Information S1).

We observed increasing T_{opt} trends for vegetation activities across all biomes and most climatic zones (Figures 2a and 2b). The sharpest increase of T_{opt} for NDVI occurred in the polar region, with a slope of 0.18°C yr^{-1} ($R^2 = 0.71$, $p < 0.001$). Similarly, the mean T_{opt} in continent zones increased by 0.11°C per year during the study period ($R^2 = 0.7$, $p < 0.001$). Wet ecosystems in tropical and temperate regions exhibited smaller but significant increases in mean T_{opt}, while arid and dry temperature zones did not show significant increases. Among different biomes, the most rapid T_{opt} increase was observed in DNF (slope = 0.19°C yr^{-1}, $p < 0.001$), followed by SHR (slope = 0.14°C yr^{-1}, $p < 0.001$). Notably, shrubland T_{opt} increased more sharply in the boreal regions, while arid SHR showed a smaller increase (Figure S13 in Supporting Information S1). Conversely, T_{opt} in GRA and CRO exhibited less pronounced increases than forests.

10.1029/2024EF004489

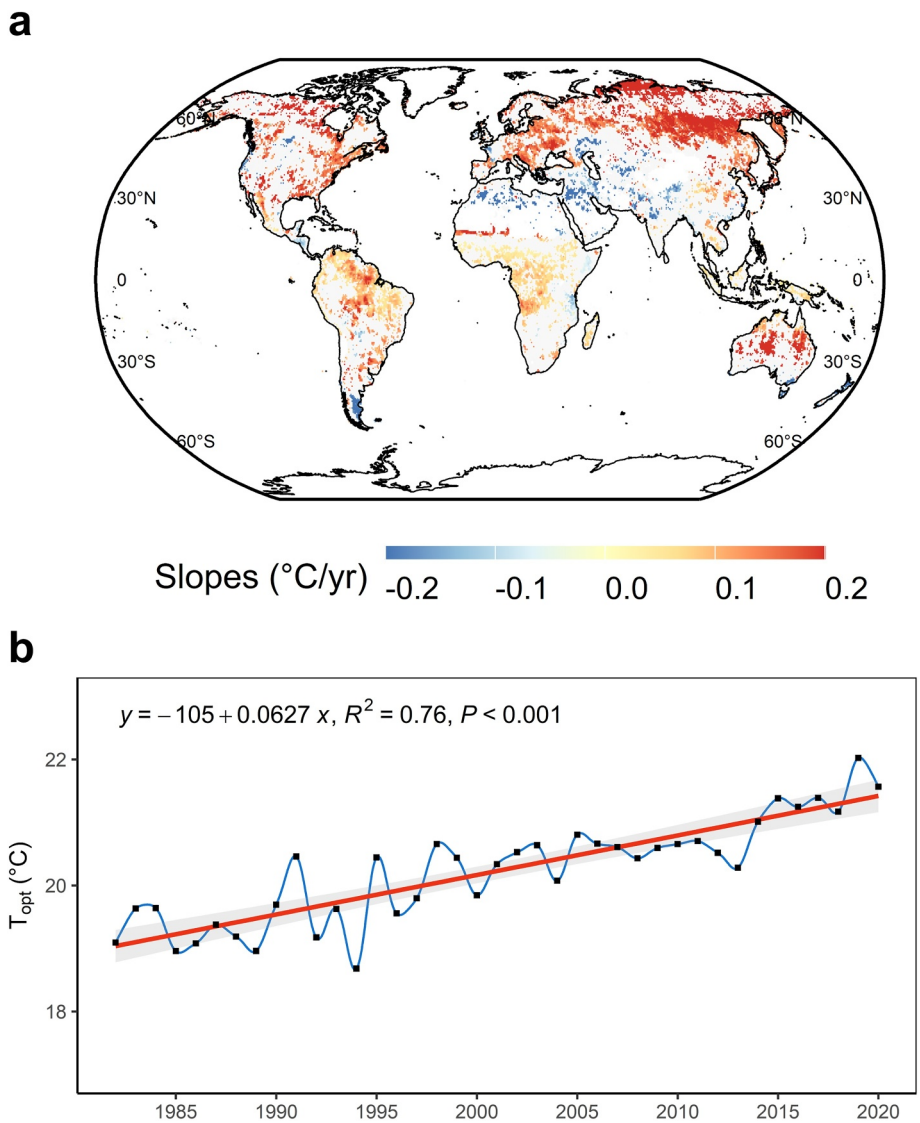

Figure 1. Spatial distribution of T_{opt} trend for vegetation activity during 1982–2020 (a). The color legend indicates the significant slopes of T_{opt} ($p < 0.05$). White areas indicate non-vegetated areas, while gray areas indicate insignificant trends. The temporal trend of globally averaged T_{opt} for vegetation activity (b). The blue line is the line plot of the global average $T_{opt,}$ while the red line represents the linear fitting result.

3.2. Thermal Acclimation of T_{opt} With Increasing Temperatures

T_{opt} of vegetation activity showed positive correlations with T_{max} globally (Figure 3a, $p < 0.05$), indicating that the increase in T_{opt} closely tracked temperature changes. Across vegetated areas, 30.1% displayed significant positive correlations ($p < 0.05$) between T_{opt} for NDVI and T_{max}, while 3.8% exhibited negative correlations. Significant positive correlations were observed in various regions across Asia, Europe, South America, and North America. Tropical regions showed the strongest correlations, followed by continental and polar areas (Figure 3b). In contrast, dry temperate and arid ecosystems displayed weaker correlations, with some arid ecosystems showing negative correlations. Among different biomes, the most significant correlations were found in EBF, while GRA, SHR, and CRO showed weaker correlations (Figure 2c). In addition, T_{opt} of tropical forests was found to be more sensitive to T_{max} changes than that of temperate forests (Figure S14 in Supporting Information S1). We further tested the correlations between T_{opt} and mean daily maximum temperatures, and found highly consistent results (Figure S15 in Supporting Information S1). Additionally, the T_{opt} derived using the binned method, AVHRR

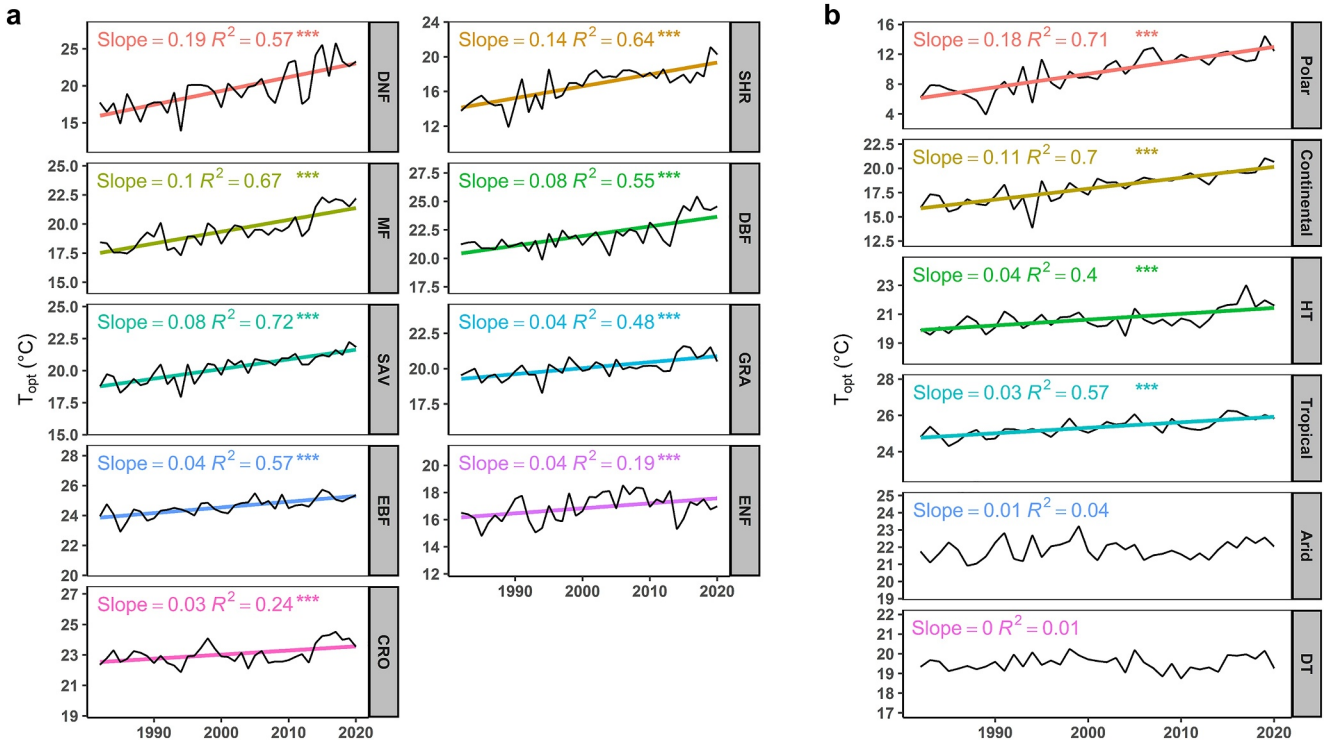

Figure 2. Temporal trends of averaged T_{opt} across biomes (a) and climate zones (b). Solid linear lines indicate significant linear trends over the years. HT, Hot temperate; DT, Dry temperate; Significance levels: $p < 0.001$, ***.

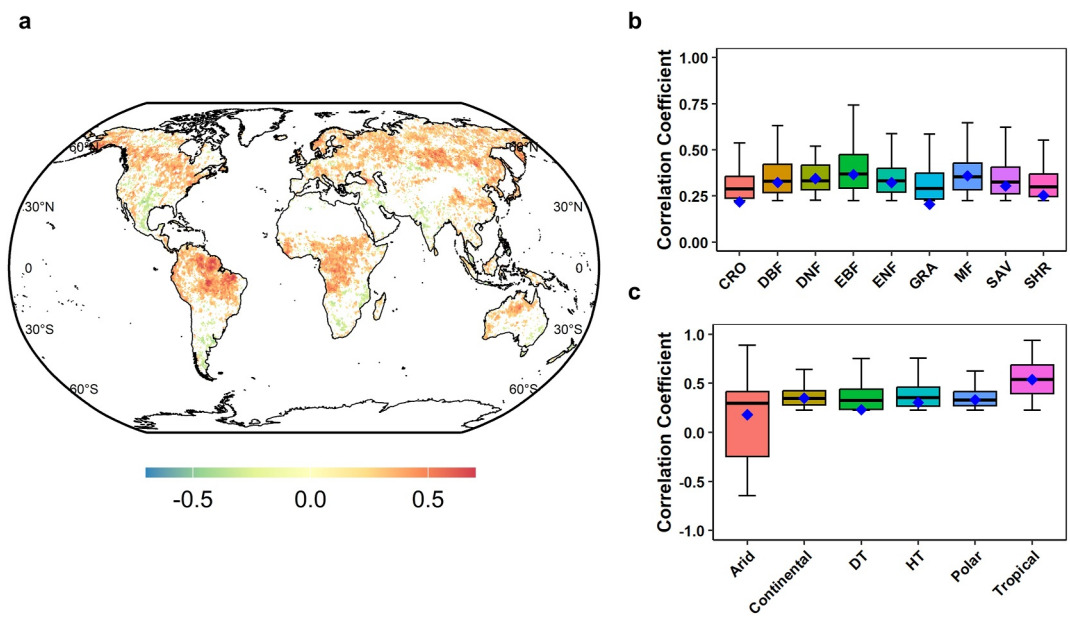

Figure 3. Spatial distribution of significant correlation coefficient (R) values between T_{opt} and T_{max} during 1982–2020 (a), and the average correlation coefficient in different climate zones (b) and vegetation types (c). The maximum and minimum extents of the colored boxes in panels (b, c) indicate the 25th and 75th percentiles and the whiskers represent the 5th and 95th percentiles, respectively. HT, Humid temperate; DT, Dry temperate.

10.1029/2024EF004489

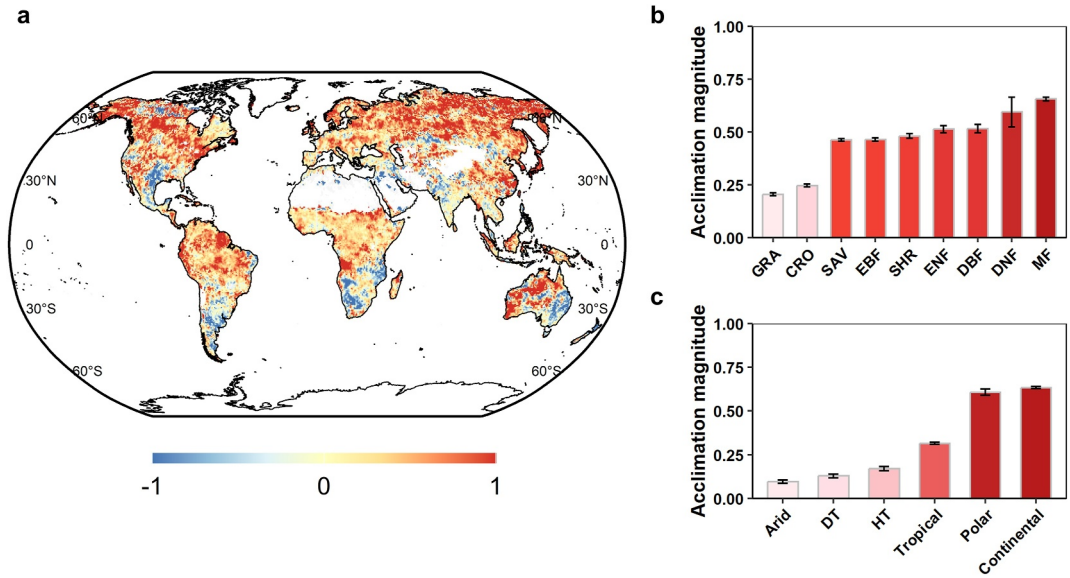

Figure 4. The spatial distribution of thermal acclimation magnitude of vegetation activity during 1982–2020 (a). The slopes refer to the partial regression slope between T_{opt} for Normalized Difference Vegetation Index and T_{max} while accounting for the effects of precipitation and light. White areas indicate non-vegetated regions. Thermal acclimation magnitude among biomes (b) and climate zones (c). The error bars refer to the standardized deviations. HT, Humid temperate; DT, Dry temperate.

NIRv, and FLUXCOM GPP data sets also exhibited significant positive correlations with T_{max} (Figure S16–18 in Supporting Information S1), highlighting the universality of thermal acclimation.

3.3. Thermal Acclimation Magnitude of Vegetation Activity

The thermal acclimation magnitude of different ecosystems was determined by calculating the changes in T_{opt} in response to T_{max} changes ($\delta T_{opt}/\delta T_{max}$). We found that the global average thermal acclimation magnitude for NDVI was 0.38°C per 1°C. Generally, Continental and polar regions exhibited the highest thermal acclimation magnitudes, with mean values of $\delta T_{opt}/\delta T_{max}$ at 0.63°C/1°C and 0.6°C/1°C, respectively (Figure 4c). In addition, tropical vegetations showed a larger acclimation magnitude than temperate vegetations (Figure 4c, Figure S19 in Supporting Information S1). Conversely, the acclimation magnitudes were considerably smaller in the arid ecosystems, with mean values of 0.03°C/1°C. Regarding biomes, MF demonstrated the greatest acclimation magnitude ($\delta T_{opt}/\delta T_{max}$ = 0.65°C/1°C), followed by DNF ($\delta T_{opt}/\delta T_{max}$ = 0.59°C/1°C). While boreal forests showed the largest acclimation magnitude, tropical forests exhibited greater acclimation capability than temperate forests (Figure S19 in Supporting Information S1). In addition, forest ecosystems generally exhibited larger acclimation capacities than non-forest biomes (Figure 4c).

To test the robustness of the acclimation magnitudes, we repeated our analysis with mean daily maximum temperatures and found consistent results (Figure S20 in Supporting Information S1). The magnitude of T_{opt} acclimation to mean daily maximum temperatures was slightly larger than that to T_{max}, indicating that temperature optima of global ecosystems might be more sensitive to changes in annual mean temperatures. In addition, we also repeated our analysis using the T_{opt} for NIRv and FLUXCOM GPP, and the T_{opt} for NDVI derived by the binned method, respectively. The results reveal similar acclimation magnitudes for T_{opt} of different vegetation indices (Figures S21–S23 in Supporting Information S1). Overall, these results suggested that the acclimation magnitudes of vegetation activity found in this study were comparable between different T_{opt} extraction methods and vegetation indices.

3.4. Determinants of Thermal Acclimation Magnitude

The acclimation magnitude was mainly influenced by temperature variabilities (CV) and water deficits (VPD and SWC) (Figure 5a). In addition, partial dependency analysis revealed that the acclimation magnitude increased

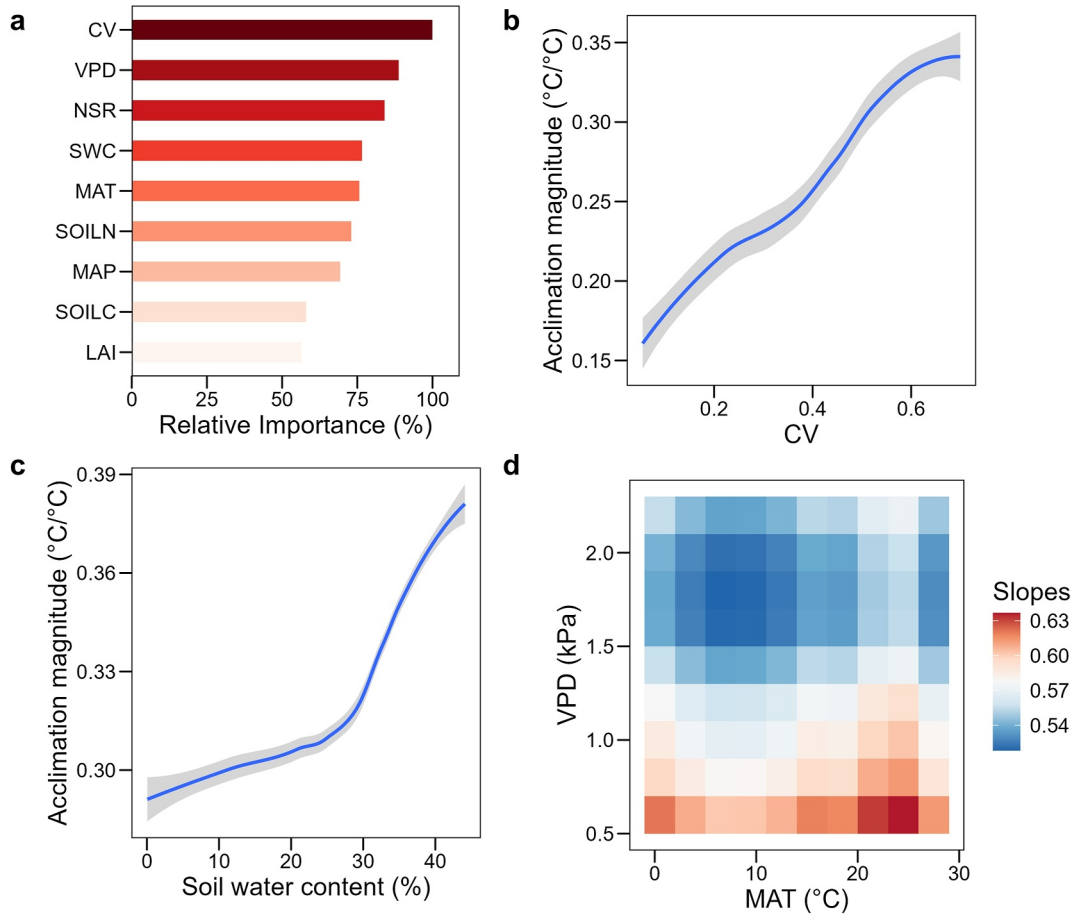

Figure 5. The relative importance of different predictors in determining the thermal acclimation magnitude of vegetation activity and climatic variables across grids (a), and the relationships between thermal acclimation magnitude of vegetation activity and mean annual temperature CV (b), soil water content (c), and vapor pressure deficit (d). The relative importance for a specific variable was calculated as the ratio of its importance in the model divided by the maximum importance (the importance of CV in the model) in percentages. The blue lines represent fitting lines by the locally estimated scatterplot smoothing method.

with rising temperature variability and SWC (Figures 5b and 5c). In contrast, given the collinearity between VPD and MAT, we employed a two-way partial dependency regression method to decouple the influence of VPD and MAT on the acclimation magnitude (Figure 5d). The results showed that an increase in VPD decreased the acclimation magnitude, while an increase in MAT generally augmented the acclimation magnitude to a critical point, beyond which the acclimation magnitude started to decline.

4. Discussion

In this study, we revealed that the T_{opt} of the global vegetation activity has significantly increased over the past four decades. The increase in T_{opt} closely tracked the increase in air temperatures, demonstrating that global ecosystems are able to acclimate to a warming climate by shifting their temperature responses. This phenomenon has been mostly reported in leaf-scale warming experiments and species-level observations (Björkman et al., 1978; Scafaro et al., 2017; Yamori et al., 2014). Our research extends the understanding of thermal acclimation to a global context, showing that terrestrial ecosystems have been undergoing significant thermal acclimation under current warming scenarios. Moreover, our results show that the acclimation magnitudes of vegetation activity vary significantly across biomes and climatic zones, which are mainly influenced by water deficits and interannual temperature variability. The global pattern of acclimation magnitudes is crucial for estimating future T_{opt} in a warming climate and can be used as an important benchmark for evaluating the accuracy of earth system models (ESMs).

4.1. Thermal Acclimation on a Global Scale

We found that global T_{opt} increased significantly during 1982–2020. The observed increase in T_{opt} was correlated strongly with rising T_{max} (Figure 3), indicating thermal acclimation at the ecosystem level. Such acclimation responses have been well-documented at the leaf and species levels (Björkman et al., 1978; Yamori et al., 2014). Our results not only extend the concept of photosynthetic acclimation to a global scale but also reveal that ecosystem acclimation has widely occurred under the current warming magnitude. These findings are partly supported by observations across eddy-covariance sites (Niu et al., 2012; Wang et al., 2023). However, previous studies have not documented a specific increase in T_{opt} over time (Wang et al., 2023), probably because the FLUXNET data set covers a short period, and T_{max} does not consistently rise year-over-year in those studies. Similarly, Huang et al. (2019) observed minimal changes in T_{opt} across years using biweekly NDVI data and a moving window of 10 years. The biweekly data smooths out NDVI variations, which may result in a significant underestimation of T_{opt} changes if the peak NDVI occurs in the same week in one year and another. In addition, our study employed a year-to-year analysis instead of the moving window approach. The year-to-year analysis increases the interannual variability of NDVI, thereby increasing the probability of detecting changes in T_{opt}.

Leaf-level experiments have indicated that thermal acclimation is mainly due to increased Rubisco activity and electron transport capability (Sage & Kubien, 2007; Scafaro et al., 2017). However, at the ecosystem level, the increase in T_{opt} may also be related to processes other than leaf-level carboxylation. For instance, elevated temperatures may facilitate root growth (Malhotra et al., 2020; Wang et al., 2021), thereby enhancing water accessibility and promoting vegetation activity under high temperatures. Additionally, warming may increase the availability of nitrogen and phosphorus through increased mineralization, which in turn boosts plant activity in warmer years (Hobbie & Chapin III, 1998).

We found that, on a global scale, T_{opt} of vegetation activity increased by 0.38°C per 1°C increase in T_{max}. This acclimation magnitude was significantly smaller than that derived from spatial gradients (Huang et al., 2019; Wang et al., 2023), indicating that the spatial sensitivity of T_{opt} to T_{max} cannot be directly used to predict future T_{opt} changes. Moreover, the acclimation magnitude was also smaller than that observed at the species level. For instance, Gunderson et al. (2010) reported acclimation magnitudes ranging from 0.51°C to 1.07°C/1°C for five deciduous tree species. Similarly, Slot and Winter (2017) found an acclimation magnitude of 0.47°C/1°C for three wet tropical forest tree seedlings. However, our study captures the acclimation of T_{opt} at the ecosystem level, offering a broader perspective that reflects the warming response of vegetation communities. This suggests that the sensitivity of ecosystem productivity to warming may differ from that observed at the species level, highlighting the need to incorporate ecosystem-level experiments into projections of global vegetation productivity under warming.

4.2. Variations in Thermal Acclimation Among Climate Zones and Biomes

Ecosystems in different climate types showed great variations in their T_{opt} trends. Polar regions exhibited the sharpest increase in T_{opt}, which agrees with the previous study (Huang et al., 2019) and can be attributed to the most significant temperature increases in these regions (Brown et al., 2017; Xu et al., 2013). Moreover, our findings indicate that the largest T_{opt} increase in polar regions is associated with large acclimation capacities (Figure 4c), aligning with a previous study on boreal tree species (Sendall et al., 2015). This high acclimation capacity in polar ecosystems is likely driven by their substantial interannual temperature variability (Figure S24 in Supporting Information S1), which may enable these ecosystems to adjust more effectively to sustained warming. Additionally, warming may strongly facilitate nitrogen mineralization in polar regions, thereby enhancing vegetation activity (Rustad et al., 2001). Furthermore, warming could also induce a rapid shift in species compositions towards more productive functional groups (i.e., an increase of deciduous shrubs) in the polar region, which enhances vegetation activities at higher temperatures (Chapin III et al., 1995). Conversely, we observed a few negative correlations between T_{opt} and T_{max} in forest-tundra transitions in northern Canada, possibly due to increased drying and wildfires under warming in these regions, which have been shown to reduce plant growth and photosynthesis (Olthof et al., 2008; Stocks, 1993; Zhang et al., 2015).

Similarly, ecosystems with a continental climate exhibited a large increase in T_{opt} and the largest acclimation capacity (Figure 4c). The continental climate is characterized by hot summers and cold winters, with significant temperature variations across the seasons. Thus, continental plants may better adjust to temperature change. Moreover, previous studies have shown that prolonged exposure to warming may facilitate continental species to

produce new leaves with the chemical composition and enzymatic machinery necessary for more complete acclimation (Loveys et al., 2003).

In addition, we found that tropical ecosystems have a higher acclimation capacity than temperate ecosystems, which is supported by a previous study showing a larger adjustment of T_{opt} in tropic forest species than in temperate species (Choury et al., 2022). This can be explained by a strong temperature response of RuBP carboxylation capability in tropical species (Hikosaka et al., 2006). However, it is worth noting that the temperature range experienced by the tropical ecosystems during the course of our study period is considerably lower than that projected in most warming experiments. Therefore, with the continuation of the observed warming trend, tropical forests are likely to exceed their temperature tolerance thresholds, with further temperature increases potentially reducing vegetation growth (Doughty et al., 2023).

In contrast, dry ecosystems exhibited a relatively small increase in T_{opt}. This is likely due to that vegetation activities in these ecosystems are strongly limited by water deficits associated with elevated temperatures (Wang et al., 2022), which mitigates the positive effect of warming on T_{opt}. In regions with the lowest precipitation levels, an increase in T_{max} can even negatively impact T_{opt} (Figure 3c, and Figure S13 in Supporting Information S1), probably because elevated VPD with warming significantly reduces stomatal conductance, which in turn inhibits plant activity at higher temperatures (Yuan et al., 2019). Therefore, further studies should investigate how T_{opt} responds to combined warming and dry conditions to better estimate thermal acclimation in dry areas.

Among the various biomes, MF and EBF showed the strongest acclimation capacities (Figure 4b). This is likely due to the fact that evergreen species have longer life spans and retain their leaves throughout the year (Chabot & Hicks, 1982). This prolonged exposure to fluctuating temperatures allows them to progressively adapt to warmer temperatures. In contrast, non-forest ecosystems exhibited a lower thermal acclimation magnitude than forests, which may be related to the lower temperature homeostasis of photosynthetic activity and shorter life spans (Yamori et al., 2014). Additionally, the weak thermal acclimation capacity in grasslands may be attributed to their lower water levels, which constrains the potential for increased maximum plant assimilation capabilities (Wang et al., 2023). In particular, in arid GRA and SHR, increased water limitation and heat-induced damage to plant physiology may largely restrict the increase in plant photosynthesis, thereby limiting the capacity of these ecosystems to cope with warming (Hoover et al., 2014; Morgan et al., 2004). In contrast, SHR in boreal regions exhibited a high acclimation capacity (Figure S19 in Supporting Information S1), likely because these ecosystems are located in the northernmost areas, where they experience more rapid warming. Such exposure to intense temperature changes can result in rapid shifts in species composition (e.g., increase the abundance of high shrubs) and derive the selection of traits, enabling photosynthetic activity to further increase under high temperatures (Oechel et al., 2000; Post et al., 2009; Walker et al., 2006). In conclusion, the observed variations in T_{opt} trends and thermal acclimation capacities reflect that different climate types and biomes have complex adjustment and adaptation strategies to cope with warming. Moreover, our findings suggest that polar and continental ecosystems may be more efficient at adapting to warming, which will ultimately benefit species survival and productivity in these regions.

4.3. Divers for Thermal Acclimation Magnitudes, Uncertainties and Implications

The acclimation magnitude was determined mainly by temperature variability, which is supported by species-level experiments (Berry & Bjorkman, 1980; Cunningham & Read, 2002). A higher degree of temperature variability reflects that ecosystems have experienced a greater range of temperature fluctuations. Therefore, they may be better equipped to adapt to warmer temperatures. However, it is worth noting that surface air temperature variability may potentially decline in the future (Brown et al., 2017). Thus, the positive impact of warming on T_{opt} may be less pronounced. In addition, we found water deficits (high VPD and low SWC) significantly reduced acclimation magnitudes, which is in line with a previous study on T_{opt} for GPP (Wang et al., 2023). This is because plants residing in high-water stress areas may adopt a water-conserving strategy by closing stomata under higher temperatures to reduce water loss (Osakabe et al., 2014), thereby reducing vegetation activity. This finding suggests that the anticipated increases in T_{opt} in global ecosystems may be dampened in the future due to trends of rising VPD and decreasing soil moisture (Fang et al., 2022; Zhou et al., 2021).

While our study provides robust evidence for the rising T_{opt} of vegetation activity, certain uncertainties remain. One major source of uncertainty is the accuracy of satellite-derived indices. For instance, the orbital drift of satellites carrying AVHRR sensors leads to large uncertainties in NDVI prior to 2000 due to differences in solar

zenith angle (Frankenberg et al., 2021; Nagol et al., 2014). To test whether these errors affected the estimates of T_{opt}, we compared NDVI-derived T_{opt} with site observations during the pre-2000 period. The results showed high correlations between T_{opt} for AVHRR NDVI and site-observed GPP, both at the mean and across years (Figure S25 in Supporting Information S1), indicating that AVHRR NDVI successfully projected the interannual variability of T_{opt} for vegetation activity despite potential uncertainties due to orbital drifts. However, we still advocate the integration of ground-based observations and the calibration of continuous satellite data to improve estimates for vegetation temperature responses. Another area for improvement is to fully explore the driving factors of the increase in T_{opt}. For instance, the extension of the photosynthetic season under warming may result in alterations to T_{opt}, due to changes in the early phenology and the timing of peak NDVI (Piao et al., 2007). Therefore, future research should also consider the influence of other environmental variables, such as soil moisture and nutrient availability, in order to develop a more comprehensive understanding of the factors affecting T_{opt} and thermal acclimation in different ecosystems.

The study has important implications for ESMs to better predict the temperature response of global vegetation. The T_{opt} is a key parameter in ecological models for predicting photosynthesis (Smith & Dukes, 2013). The observed increasing trends of T_{opt} highlight the necessity for land models to incorporate temperature acclimation processes, which are largely absent in the majority of process-based models (Smith & Dukes, 2013). In this context, previous studies have demonstrated that the omission of leaf photosynthetic and respiratory temperature acclimation in the Community Land Model will result in an underestimation of terrestrial ecosystem carbon pools by 20 Pg (22%) at the end of the 21st century and under the climate scenario Representative Concentration Pathway 8.5 (Lombardozzi et al., 2015). In contrast, Bennett et al. (2024) found that incorporating thermal acclimation functions into the CABLE model enhanced carbon uptake in tropical ecosystems but not in temperate forests across Australian wooded regions. Our results indicate that we need to account for the variations in acclimation capacities between different biomes in ESMs. Moreover, even in revised models that incorporate photosynthetic acclimation, they rely heavily on the linear response of T_{opt} to growth temperature derived from species-level experiments (Kattge & Knorr, 2007). However, this approach may not be sufficient to fully capture other ecosystem-level mechanisms. Consequently, the findings of our study on the global variation and drivers of thermal acclimation magnitude may assist in more accurately parameterizing the revised models.

5. Conclusions

We found a significant increase in T_{opt} of vegetation activities over the past four decades and revealed universal thermal acclimation to ongoing temperature increases in global vegetation. The results indicate that ecosystems have comparable capabilities to survive and function efficiently under elevated temperatures. With regrad to the global carbon cycle, the increase in T_{opt} suggests that ecosystems may have a greater potential for carbon uptake under elevated temperatures. Furthermore, we assessed the acclimation capabilities in different climate types and biomes and found that polar and continental climate zones were the hotspots where vegetation activity displayed the strongest thermal acclimation. These findings are of significant importance for the parameterization of temperature responses in ESMs.

Data Availability Statement

All the data sources used for this analysis were publicly available. The AVHRR NDVI used in this study was available in Vermote et al. (2014). NASA's MERRA2 temperature data were available in Global Modeling and Assimilation Office (2015). The ERA5-land data sets were available in Muñoz-Sabater et al. (2021). The MODIS Landcover type map can be found in Friedl and Sulla-Menashe (2019). The MODIS LAI data set was available in Myneni et al. (2015). The ecoregions were defined by KÖPPEN-GEIGER climate classification, which could be found in Kottek et al. (2006). The analyses were conducted in *R* with package *mblm*, *nlme*, and *randomForest* (Komsta, 2013; Pinheiro et al., 2017; RColorBrewer & Liaw, 2018).

Acknowledgments
This work was financially supported by the National Key *R* and *D* Program of China (2022YFF0802102), the National Natural Science Foundation of China (31988102), and the international collaboration project of the Chinese Academy of Sciences (177GJHZ2022020BS).

References

Badgley, G., Field, C. B., & Berry, J. A. (2017). Canopy near-infrared reflectance and terrestrial photosynthesis. *Science Advances*, *3*(3), e1602244. https://doi.org/10.1126/sciadv.1602244

Battaglia, M., Beadle, C., & Loughhead, S. (1996). Photosynthetic temperature responses of Eucalyptus globulus and Eucalyptus nitens. *Tree Physiology*, *16*(1–2), 81–89. https://doi.org/10.1093/treephys/16.1-2.81

Beck, H. E., McVicar, T. R., van Dijk, A. I., Schellekens, J., de Jeu, R. A., & Bruijnzeel, L. A. (2011). Global evaluation of four AVHRR–NDVI data sets: Intercomparison and assessment against Landsat imagery. *Remote Sensing of Environment*, *115*(10), 2547–2563. https://doi.org/10.1016/j.rse.2011.05.012

Bennett, A. C., Knauer, J., Bennett, L. T., Haverd, V., & Arndt, S. K. (2024). Variable influence of photosynthetic thermal acclimation on future carbon uptake in Australian wooded ecosystems under climate change. *Global Change Biology*, *30*(1), e17021. https://doi.org/10.1111/gcb.17021

Berry, J., & Bjorkman, O. (1980). Photosynthetic response and adaptation to temperature in higher plants. *Annual Review of Plant Physiology*, *31*(1), 491–543. https://doi.org/10.1146/annurev.pp.31.060180.002423

Björkman, O., Badger, M., & Armond, P. A. (1978). *Thermal acclimation of photosynthesis: Effect of growth temperature on photosynthetic characteristics and components of the photosynthetic apparatus in nerium oleander* (Vol. 77, pp. 262–276). Carnegie Institution of Washington Yearbook.

Brown, P. T., Ming, Y., Li, W., & Hill, S. A. (2017). Change in the magnitude and mechanisms of global temperature variability with warming. *Nature Climate Change*, *7*(10), 743–748. https://doi.org/10.1038/nclimate3381

Chabot, B. F., & Hicks, D. J. (1982). The ecology of leaf life spans. *Annual Review of Ecology and Systematics*, *13*(1), 229–259. https://doi.org/10.1146/annurev.es.13.110182.001305

ChapinIII, F. S., Shaver, G. R., Giblin, A. E., Nadelhoffer, K. J., & Laundre, J. A. (1995). Responses of arctic tundra to experimental and observed changes in climate. *Ecology*, *76*(3), 694–711. https://doi.org/10.2307/1939337

Chen, J., Jönsson, P., Tamura, M., Gu, Z., Matsushita, B., & Eklundh, L. (2004). A simple method for reconstructing a high-quality NDVI time-series data set based on the Savitzky–Golay filter. *Remote Sensing of Environment*, *91*(3–4), 332–344. https://doi.org/10.1016/j.rse.2004.03.014

Choury, Z., Wujeska-Klause, A., Bourne, A., Bown, N. P., Tjoelker, M. G., Medlyn, B. E., & Crous, K. Y. (2022). Tropical rainforest species have larger increases in temperature optima with warming than warm-temperate rainforest trees. *New Phytologist*, *234*(4), 1220–1236. https://doi.org/10.1111/nph.18077

Crous, K. Y., Uddling, J., & De Kauwe, M. G. (2022). Temperature responses of photosynthesis and respiration in evergreen trees from boreal to tropical latitudes. *New Phytologist*, *234*(2), 353–374. https://doi.org/10.1111/nph.17951

Cunningham, S., & Read, J. (2002). Comparison of temperate and tropical rainforest tree species: Photosynthetic responses to growth temperature. *Oecologia*, *133*(2), 112–119. https://doi.org/10.1007/s00442-002-1034-1

Doughty, C. E., Keany, J. M., Wiebe, B. C., Rey-Sanchez, C., Carter, K. R., Middleby, K. B., et al. (2023). Tropical forests are approaching critical temperature thresholds. *Nature*, *621*(7977), 105–111. https://doi.org/10.1038/s41586-023-06391-z

Fang, J., Piao, S., He, J., & Ma, W. (2004). Increasing terrestrial vegetation activity in China, 1982–1999. *Science in China Series C: Life Sciences*, *47*(3), 229–240. https://doi.org/10.1007/bf03182768

Fang, Z., Zhang, W., Brandt, M., Abdi, A. M., & Fensholt, R. (2022). Globally increasing atmospheric aridity over the 21st century. *Earth's Future*, *10*(10), e2022EF003019. https://doi.org/10.1029/2022ef003019

Frankenberg, C., Yin, Y., Byrne, B., He, L., Gentine, P., Zha, J., et al. (2021). Comment on "Recent global decline of CO_2 fertilization effects on vegetation photosynthesis". *Science*, *373*(6562), eabg2947. https://doi.org/10.1126/science.abg5673

Friedl, M., & Sulla-Menashe, D. (2019). MCD12Q1 MODIS/Terra+Aqua land cover type yearly L3 global 500m SIN grid V006 [Dataset]. *NASA EOSDIS Land Processes Distributed Active Archive Center*. https://doi.org/10.5067/MODIS/MCD12Q1.006

Global Modeling and Assimilation Office, G. (2015). MERRA-2 tavg1_2d_slv_Nx: 2d,1-Hourly,Time-Averaged,Single-Level,Assimilation, Single-Level diagnostics V5.12.4 [Dataset]. *Goddard Earth Sciences Data and Information Services Center (GES DISC)*. Retrieved from https://data.nasa.gov/dataset/MERRA-2-tavg1_2d_slv_Nx-2d-1-Hourly-Time-Averaged-/srpu-epqr

Grossiord, C., Buckley, T. N., Cernusak, L. A., Novick, K. A., Poulter, B., Siegwolf, R. T., et al. (2020). Plant responses to rising vapor pressure deficit. *New Phytologist*, *226*(6), 1550–1566. https://doi.org/10.1111/nph.16485

Gunderson, C. A., O'hara, K. H., Campion, C. M., Walker, A. V., & Edwards, N. T. (2010). Thermal plasticity of photosynthesis: The role of acclimation in forest responses to a warming climate. *Global Change Biology*, *16*(8), 2272–2286. https://doi.org/10.1111/j.1365-2486.2009.02090.x

Hikosaka, K., Ishikawa, K., Borjigidai, A., Muller, O., & Onoda, Y. (2006). Temperature acclimation of photosynthesis: Mechanisms involved in the changes in temperature dependence of photosynthetic rate. *Journal of Experimental Botany*, *57*(2), 291–302. https://doi.org/10.1093/jxb/erj049

Hobbie, S. E., & ChapinIII, F. S. (1998). The response of tundra plant biomass, aboveground production, nitrogen, and CO_2 flux to experimental warming. *Ecology*, *79*(5), 1526–1544. https://doi.org/10.2307/176774

Hoover, D. L., Knapp, A. K., & Smith, M. D. (2014). Resistance and resilience of a grassland ecosystem to climate extremes. *Ecology*, *95*(9), 2646–2656. https://doi.org/10.1890/13-2186.1

Huang, K., Xia, J., Wang, Y., Ahlström, A., Chen, J., Cook, R. B., et al. (2018). Enhanced peak growth of global vegetation and its key mechanisms. *Nature ecology & evolution*, *2*(12), 1897–1905. https://doi.org/10.1038/s41559-018-0714-0

Huang, M., Piao, S., Ciais, P., Peñuelas, J., Wang, X., Keenan, T. F., et al. (2019). Air temperature optima of vegetation productivity across global biomes. *Nature ecology & evolution*, *3*(5), 772–779. https://doi.org/10.1038/s41559-019-0838-x

Hughes, L. (2000). Biological consequences of global warming: Is the signal already apparent? *Trends in Ecology & Evolution*, *15*(2), 56–61. https://doi.org/10.1016/s0169-5347(99)01764-4

Jung, M., Reichstein, M., Schwalm, C. R., Huntingford, C., Sitch, S., Ahlström, A., et al. (2017). Compensatory water effects link yearly global land CO_2 sink changes to temperature. *Nature*, *541*(7638), 516–520. https://doi.org/10.1038/nature20780

Jung, M., Schwalm, C., Migliavacca, M., Walther, S., Camps-Valls, G., Koirala, S., et al. (2020). Scaling carbon fluxes from eddy covariance sites to globe: Synthesis and evaluation of the FLUXCOM approach. *Biogeosciences*, *17*(5), 1343–1365. https://doi.org/10.5194/bg-17-1343-2020

Kattge, J., & Knorr, W. (2007). Temperature acclimation in a biochemical model of photosynthesis: A reanalysis of data from 36 species. *Plant, Cell and Environment*, *30*(9), 1176–1190. https://doi.org/10.1111/j.1365-3040.2007.01690.x

Komsta, L. (2013). MBLM: Median-based linear models [Software]. *R package version 0*, *12*, 1. https://cran.r-project.org/web/packages/mblm/index.html

Kottek, M., Grieser, J., Beck, C., Rudolf, B., & Rubel, F. (2006). World map of the Köppen-Geiger climate classification updated [Dataset]. https://doi.org/10.5194/hess-11-1633-2007

Kumarathunge, D. P., Medlyn, B. E., Drake, J. E., Tjoelker, M. G., Aspinwall, M. J., Battaglia, M., et al. (2019). Acclimation and adaptation components of the temperature dependence of plant photosynthesis at the global scale. *New Phytologist*, *222*(2), 768–784. https://doi.org/10.1111/nph.15668

Lian, X., Piao, S., Chen, A., Huntingford, C., Fu, B., Li, L. Z., et al. (2021). Multifaceted characteristics of dryland aridity changes in a warming world. *Nature Reviews Earth and Environment*, *2*(4), 232–250. https://doi.org/10.1038/s43017-021-00144-0

Lin, Y.-S., Medlyn, B. E., & Ellsworth, D. S. (2012). Temperature responses of leaf net photosynthesis: The role of component processes. *Tree Physiology*, *32*(2), 219–231. https://doi.org/10.1093/treephys/tpr141

Lloyd, J., & Farquhar, G. D. (2008). Effects of rising temperatures and [CO_2] on the physiology of tropical forest trees. *Philosophical Transactions of the Royal Society B: Biological Sciences*, *363*(1498), 1811–1817. https://doi.org/10.1098/rstb.2007.0032

Lombardozzi, D. L., Bonan, G. B., Smith, N. G., Dukes, J. S., & Fisher, R. A. (2015). Temperature acclimation of photosynthesis and respiration: A key uncertainty in the carbon cycle-climate feedback. *Geophysical Research Letters*, *42*(20), 8624–8631. https://doi.org/10.1002/2015gl065934

Loveys, B., Atkinson, L. J., Sherlock, D., Roberts, R. L., Fitter, A. H., & Atkin, O. K. (2003). Thermal acclimation of leaf and root respiration: An investigation comparing inherently fast-and slow-growing plant species. *Global Change Biology*, *9*(6), 895–910. https://doi.org/10.1046/j.1365-2486.2003.00611.x

Malhotra, A., Brice, D. J., Childs, J., Graham, J. D., Hobbie, E. A., Vander Stel, H., et al. (2020). Peatland warming strongly increases fine-root growth. *Proceedings of the National Academy of Sciences* (Vol. 117(30), 17627–17634). https://doi.org/10.1073/pnas.2003361117

Masson-Delmotte, V., Zhai, P., Pirani, A., Connors, S. L., Péan, C., Berger, S., et al. (2021). Climate change 2021: The physical science basis. In *Contribution of working group I to the sixth assessment report of the intergovernmental panel on climate change* (Vol. 2).

Morgan, J., Pataki, D., Körner, C., Clark, H., Del Grosso, S., Grünzweig, J., et al. (2004). Water relations in grassland and desert ecosystems exposed to elevated atmospheric CO_2. *Oecologia*, *140*(1), 11–25. https://doi.org/10.1007/s00442-004-1550-2

Muñoz-Sabater, J., Dutra, E., Agustí-Panareda, A., Albergel, C., Arduini, G., Balsamo, G., et al. (2021). ERA5-Land: A state-of-the-art global reanalysis dataset for land applications. *Earth System Science Data*, *13*(9), 4349–4383. https://doi.org/10.5194/essd-13-4349-2021

Myneni, R., Knyazikhin, Y., & Park, T. (2015). MOD15A2H MODIS/terra leaf area index/FPAR 8-day L4 global 500m SIN grid V006 [Dataset]. *NASA EOSDIS Land Processes Distributed Active Archive Center*. https://doi.org/10.5067/MODIS/MOD15A2H.006

Nagol, J. R., Vermote, E. F., & Prince, S. D. (2014). Quantification of impact of orbital drift on inter-annual trends in AVHRR NDVI data. *Remote Sensing*, *6*(7), 6680–6687. https://doi.org/10.3390/rs6076680

Niinemets, Ü. (2001). Global-scale climatic controls of leaf dry mass per area, density, and thickness in trees and shrubs. *Ecology*, *82*(2), 453–469. https://doi.org/10.2307/2679872

Niu, S., Li, Z., Xia, J., Han, Y., Wu, M., & Wan, S. (2008). Climatic warming changes plant photosynthesis and its temperature dependence in a temperate steppe of northern China. *Environmental and Experimental Botany*, *63*(1–3), 91–101. https://doi.org/10.1016/j.envexpbot.2007.10.016

Niu, S., Luo, Y., Fei, S., Yuan, W., Schimel, D., Law, B. E., et al. (2012). Thermal optimality of net ecosystem exchange of carbon dioxide and underlying mechanisms. *New Phytologist*, *194*(3), 775–783. https://doi.org/10.1111/j.1469-8137.2012.04095.x

Oechel, W. C., Vourlitis, G. L., Hastings, S. J., Zulueta, R. C., Hinzman, L., & Kane, D. (2000). Acclimation of ecosystem CO_2 exchange in the Alaskan Arctic in response to decadal climate warming. *Nature*, *406*(6799), 978–981. https://doi.org/10.1038/35023137

Olthof, I., Pouliot, D., Latifovic, R., & Chen, W. (2008). Recent (1986-2006) vegetation-specific NDVI trends in Northern Canada from satellite data. *Arctic*, 381–394.

Osakabe, Y., Osakabe, K., Shinozaki, K., & Tran, L.-S. P. (2014). Response of plants to water stress. *Frontiers in plant science*, *5*, 86. https://doi.org/10.3389/fpls.2014.00086

Pastorello, G., Trotta, C., Canfora, E., Chu, H., Christianson, D., Cheah, Y.-W., et al. (2020). The FLUXNET2015 dataset and the ONEFlux processing pipeline for eddy covariance data. *Scientific Data*, *7*(1), 225. https://doi.org/10.1038/s41597-020-0534-3

Pedelty, J., Devadiga, S., Masuoka, E., Brown, M., Pinzon, J., Tucker, C., et al. (2007). Generating a long-term land data record from the AVHRR and MODIS instruments. In *2007 IEEE international Geoscience and remote sensing Symposium*.

Piao, S., Friedlingstein, P., Ciais, P., Viovy, N., & Demarty, J. (2007). Growing season extension and its impact on terrestrial carbon cycle in the Northern Hemisphere over the past 2 decades. *Global Biogeochemical Cycles*, *21*(3). https://doi.org/10.1029/2006gb002888

Piao, S., Wang, X., Park, T., Chen, C., Lian, X., He, Y., et al. (2020). Characteristics, drivers and feedbacks of global greening. *Nature Reviews Earth and Environment*, *1*(1), 14–27. https://doi.org/10.1038/s43017-019-0001-x

Pinheiro, J., Bates, D., DebRoy, S., Sarkar, D., Heisterkamp, S., Van Willigen, B., & Maintainer, R. (2017). Package 'nlme' [Software]. *Linear and nonlinear mixed effects models, version*, *3*(1), 274. https://cran.r-project.org/web/packages/nlme/nlme.pdf

Poggio, L., De Sousa, L. M., Batjes, N. H., Heuvelink, G., Kempen, B., Ribeiro, E., & Rossiter, D. (2021). SoilGrids 2.0: Producing soil information for the globe with quantified spatial uncertainty [Dataset]. *Soils*, *7*(1), 217–240. https://doi.org/10.5194/soil-7-217-2021

Post, E., Forchhammer, M. C., Bret-Harte, M. S., Callaghan, T. V., Christensen, T. R., Elberling, B., et al. (2009). Ecological dynamics across the Arctic associated with recent climate change. *Science*, *325*(5946), 1355–1358. https://doi.org/10.1126/science.1173113

RcolorBrewer, S., & Liaw, M. A. (2018). Package 'randomforest' [Software]. *University of California*. https://cran.r-project.org/web/packages/randomForest/

Revelle, W., & Revelle, M. W. (2015). Package 'psych' [Software]. *The comprehensive R archive network*, *337*(338), 161–165. https://cran.rstudio.org/web/packages/psych/psych.pdf

Rousseeuw, P. J. (1984). Least median of squares regression. *Journal of the American Statistical Association*, *79*(388), 871–880. https://doi.org/10.1080/01621459.1984.10477105

Rustad, L., Campbell, J., Marion, G., Norby, R., Mitchell, M., Hartley, A., et al., Gcte-News. (2001). A meta-analysis of the response of soil respiration, net nitrogen mineralization, and aboveground plant growth to experimental ecosystem warming. *Oecologia*, *126*(4), 543–562. https://doi.org/10.1007/s004420000544

Sage, R. F., & Kubien, D. S. (2007). The temperature response of C3 and C4 photosynthesis. *Plant, Cell and Environment*, *30*(9), 1086–1106. https://doi.org/10.1111/j.1365-3040.2007.01682.x

Saxe, H., Cannell, M. G., Johnsen, Ø., Ryan, M. G., & Vourlitis, G. (2001). Tree and forest functioning in response to global warming. *New Phytologist*, *149*(3), 369–399. https://doi.org/10.1046/j.1469-8137.2001.00057.x

Scafaro, A. P., Xiang, S., Long, B. M., Bahar, N. H., Weerasinghe, L. K., Creek, D., et al. (2017). Strong thermal acclimation of photosynthesis in tropical and temperate wet-forest tree species: The importance of altered Rubisco content. *Global Change Biology*, *23*(7), 2783–2800. https://doi.org/10.1111/gcb.13566

Sendall, K. M., Reich, P. B., Zhao, C., Jihua, H., Wei, X., Stefanski, A., et al. (2015). Acclimation of photosynthetic temperature optima of temperate and boreal tree species in response to experimental forest warming. *Global Change Biology*, *21*(3), 1342–1357. https://doi.org/10.1111/gcb.12781

Slot, M., & Winter, K. (2017). Photosynthetic acclimation to warming in tropical forest tree seedlings. *Journal of Experimental Botany*, *68*(9), 2275–2284. https://doi.org/10.1093/jxb/erx071

Smith, N. G., & Dukes, J. S. (2013). Plant respiration and photosynthesis in global-scale models: Incorporating acclimation to temperature and CO_2. *Global Change Biology*, *19*(1), 45–63. https://doi.org/10.1111/j.1365-2486.2012.02797.x

Smith, N. G., Lombardozzi, D., Tawfik, A., Bonan, G., & Dukes, J. S. (2017). Biophysical consequences of photosynthetic temperature acclimation for climate. *Journal of Advances in Modeling Earth Systems*, *9*(1), 536–547. https://doi.org/10.1002/2016ms000732

Smith, N. G., Malyshev, S. L., Shevliakova, E., Kattge, J., & Dukes, J. S. (2016). Foliar temperature acclimation reduces simulated carbon sensitivity to climate. *Nature Climate Change*, *6*(4), 407–411. https://doi.org/10.1038/nclimate2878

Stocks, B. J. (1993). Global warming and forest fires in Canada. *The Forestry Chronicle*, *69*(3), 290–293. https://doi.org/10.5558/tfc69290-3

Sulla-Menashe, D., & Friedl, M. A. (2018). *User guide to collection 6 MODIS land cover (MCD12Q1 and MCD12C1) product* (Vol. 1, p. 18). Usgs.

Tjoelker, M., Oleksyn, J., & Reich, P. (1998). Seedlings of five boreal tree species differ in acclimation of net photosynthesis to elevated CO_2 and temperature. *Tree Physiology*, *18*(11), 715–726. https://doi.org/10.1093/treephys/18.11.715

Tramontana, G., Jung, M., Schwalm, C. R., Ichii, K., Camps-Valls, G., Ráduly, B., et al. (2016). Predicting carbon dioxide and energy fluxes across global FLUXNET sites with regression algorithms. *Biogeosciences*, *13*(14), 4291–4313. https://doi.org/10.5194/bg-13-4291-2016

Vermote, E., Justice, C., Csiszar, I., Eidenshink, J., Myneni, R., Baret, F., et al. (2014). NOAA climate data record (CDR) of normalized difference vegetation index (NDVI), version 4 [Dataset]. *NOAA National Centers for Environmental Information*. https://doi.org/10.7289/V5PZ56R6

Walker, M. D., Wahren, C. H., Hollister, R. D., Henry, G. H., Ahlquist, L. E., Alatalo, J. M., et al. (2006). Plant community responses to experimental warming across the tundra biome. *Proceedings of the National Academy of Sciences*, *103*(5), 1342–1346. https://doi.org/10.1073/pnas.0503198103

Wang, B., Chen, W., Tian, D., Li, Z., Wang, J., Fu, Z., et al. (2023). Dryness limits vegetation pace to cope with temperature change in warm regions. *Global Change Biology*, *29*(17), 4750–4757. https://doi.org/10.1111/gcb.16842

Wang, J., Defrenne, C., McCormack, M. L., Yang, L., Tian, D., Luo, Y., et al. (2021). Fine-root functional trait responses to experimental warming: A global meta-analysis. *New Phytologist*, *230*(5), 1856–1867. https://doi.org/10.1111/nph.17279

Wang, L., Jiao, W., MacBean, N., Rulli, M. C., Manzoni, S., Vico, G., & D'Odorico, P. (2022). Dryland productivity under a changing climate. *Nature Climate Change*, *12*(11), 981–994. https://doi.org/10.1038/s41558-022-01499-y

Wang, R., Gamon, J. A., Emmerton, C. A., Springer, K. R., Yu, R., & Hmimina, G. (2020). Detecting intra-and inter-annual variability in gross primary productivity of a North American grassland using MODIS MAIAC data. *Agricultural and Forest Meteorology*, *281*, 107859. https://doi.org/10.1016/j.agrformet.2019.107859

Xu, L., Myneni, R., Chapin Iii, F., Callaghan, T. V., Pinzon, J., Tucker, C. J., et al. (2013). Temperature and vegetation seasonality diminishment over northern lands. *Nature Climate Change*, *3*(6), 581–586. https://doi.org/10.1038/nclimate1836

Yamori, W., Hikosaka, K., & Way, D. A. (2014). Temperature response of photosynthesis in C 3, C 4, and CAM plants: Temperature acclimation and temperature adaptation. *Photosynthesis Research*, *119*(1–2), 101–117. https://doi.org/10.1007/s11120-013-9874-6

Yuan, W., Zheng, Y., Piao, S., Ciais, P., Lombardozzi, D., Wang, Y., et al. (2019). Increased atmospheric vapor pressure deficit reduces global vegetation growth. *Science Advances*, *5*(8), eaax1396. https://doi.org/10.1126/sciadv.aax1396

Zhang, J., Xiao, J., Tong, X., Zhang, J., Meng, P., Li, J., et al. (2022). NIRv and SIF better estimate phenology than NDVI and EVI: Effects of spring and autumn phenology on ecosystem production of planted forests. *Agricultural and Forest Meteorology*, *315*, 108819. https://doi.org/10.1016/j.agrformet.2022.108819

Zhang, Y., Wolfe, S. A., Morse, P. D., Olthof, I., & Fraser, R. H. (2015). Spatiotemporal impacts of wildfire and climate warming on permafrost across a subarctic region, Canada. *Journal of Geophysical Research: Earth Surface*, *120*(11), 2338–2356. https://doi.org/10.1002/2015jf003679

Zhou, S., Williams, A. P., Lintner, B. R., Berg, A. M., Zhang, Y., Keenan, T. F., et al. (2021). Soil moisture–atmosphere feedbacks mitigate declining water availability in drylands. *Nature Climate Change*, *11*(1), 38–44. https://doi.org/10.1038/s41558-020-00945-z